


CONDITIONS FOR THE OCCURRENCE OF INTENSE FLUXES OF ENERGETIC ELECTRONS AT $L < 1.2$ ASSOCIATED WITH SOLAR ACTIVITY AND SOLAR WIND PARAMETERS

A.V. Suvorova 
Scobeltsyn Institute of Nuclear Physics,
Lomonosov Moscow State University,
Moscow, Russia, alla_suvorova@mail.ru

A.V. Dmitriev 
Scobeltsyn Institute of Nuclear Physics,
Lomonosov Moscow State University,
Moscow, Russia, dalexav@mail.ru

Abstract. We present the results of a statistical study of transient enhancements of electrons with energies >30 keV at low drift shells in the quasi-trapped region (forbidden zone) at the geomagnetic equator. Using data from low-altitude NOAA/POES and MetOp satellites, we have compiled a catalog of events with forbidden energetic electron (FEE) enhancements for the period from 1998 to 2023. Statistical analysis of FEE events has revealed solar-cyclic, as well as seasonal and diurnal variations in the occurrence of FEE enhancements. We have examined the correlation of the annual frequency of FEE events with solar activity, solar wind parameters, and geomagnetic activity. Strong correlations have been found with the $F10.7$ index of solar activity (radio emission flux) as well as with the

Alfvén Mach number (solar wind parameter). An interpretation of the obtained results is proposed which is based on the mechanism of electrical drift and radial transport of electrons from Earth's inner radiation belt to the quasi-trapped region ($L < 1.2$). The key factor for the operation of the mechanism is the effective penetration of the electric field to low latitudes when a significant difference in the conductivity of the high-latitude ionosphere occurs in the illuminated and unilluminated sectors of local time under conditions of weakening auroral activity.

Keywords: inner radiation belt, quasi-trapped electrons, solar-terrestrial relationships.

INTRODUCTION

Electrons of Earth's radiation belt (ERB) with energies less than 1 MeV occupy the region of drift L shells, conditionally divided into outer and inner zones (Figure 1). The inner zone ($L \sim 1.2-2.5$) of energetic electrons is separated from the outer one ($L \sim 3-6$) by a narrow gap, where electron fluxes are low. The lower edge of the belt is at $L \sim 1.2$, separating ERB from the quasi-trapped zone or forbidden zone, where fluxes sharply decrease to background values. The dynamics of electrons at low drift shells ($L < 2$) is fundamentally different from their dynamics at higher ones. It has been established from satellite measurements that, unlike the outer zone, electron fluxes in the inner zone do not experience noticeable varia-

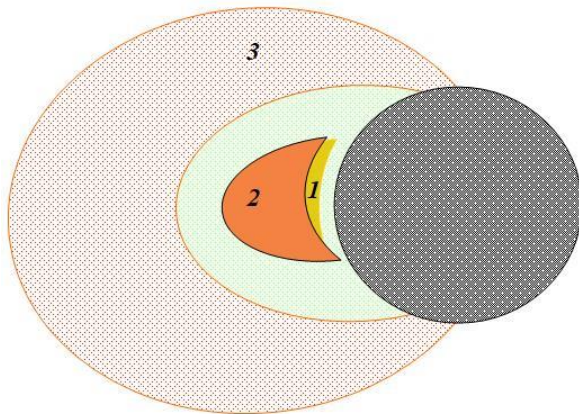


Figure 1. Structural pattern of the electron radiation belt in the energy range of tens to hundreds of keV: 1 – forbidden zone, 2 – inner ERB, 3 – outer ERB

tions caused by geomagnetic activity. Because of this, the inner zone of energetic electrons is considered quite stable. There are, nonetheless, several known cases when during very strong [Tanaka et al., 1990; Takagi et al., 1993; Gusev et al., 1995; Dmitriev, Yeh, 2008] and even moderate magnetic storms [Tadokoro et al., 2007] there were sharp and significant increases in fluxes. The formation of individual peaks in energy spectra (zebra stripes) near the lower edge of the belt ($L \sim 1.2-1.4$) can also be attributed to the unusual dynamics of inner ERB [Imhof et al., 1973; Pinto et al., 1991; Kudela et al., 1992; Sauvaud et al., 2006; Sun et al., 2024].

The unusual dynamics of inner ERB leads to another poorly studied phenomenon, in which trapped electrons with an energy 30–300 keV penetrate into very low shells $L < 1.2$, falling into the forbidden zone (1 in Figure 1) [Suvorova et al., 2012, 2014]. The flux of quasi-trapped electrons under the belt at the equator and in the $\pm 30^\circ$ latitude range sharply increases locally by several orders of magnitude as compared to the background. Due to eastward azimuthal drift of electrons, the increased flux is sequentially observed at other longitudes until it reaches the region of the South Atlantic Anomaly (SAA). In this phenomenon, the quasi-trapped electrons in the forbidden zone are called forbidden energetic electrons (FEE). Sporadic enhancements of the quasi-trapped electron flux occurred near the equator at altitudes from 300 to 800 km [Savenko et al., 1962; Heikkila, 1971; Evans, 1988; Asikainen, Mursula, 2005; Suvorova et al., 2012; Suvorova, Dmitriev, 2015]. While the phenomenon was discovered in early experiments, it was

not studied for a long time because of very rare observations and serious criticism since it was believed that measurements with elementary imperfect instruments were erroneous [Paulikas, 1975].

Recent theoretical analysis and simulation [Lejosne, Mozer, 2016; Su et al., 2016; Selesnick et al., 2019] have shown that the detected dynamics of trapped and quasi-trapped electron fluxes on low L shells is not described by up-to-date electrodynamic models. According to the models, fluxes on low L should remain relatively stable or change little — at least not by orders of magnitude.

In recent years, the dynamics of energetic electrons on low L has been actively studied in two ways: The first involves simulating radial drift processes at $L < 2.5$ [Hua et al., 2019; Lejosne, Mozer, 2016; Lejosne et al., 2022; Selesnick et al., 2016; 2019]; the second, collecting and analyzing statistics on increases in quasi-trapped electrons at $L < 1.2$, using long-term observations by low-orbit satellites [Suvorova, Dmitriev, 2015; Suvorova, 2017]. Simulation allows us to identify shortcomings of the electrodynamic models in order to further develop new theoretical approaches. Empirical analysis is used to search for effective drivers and ambient conditions affecting the magnetosphere and ionosphere, which give rise to FEE.

In this paper, we statistically analyze enhancements of FEE fluxes with an energy >30 keV. Using data from continuous monitoring (1998–2023) of energetic charged particles by a large fleet of low-orbit NOAA satellites, we have collected fairly extensive statistics on enhancements of >30 keV quasi-trapped electrons. The statistical analysis results are employed to analyze the FEE occurrence conditions when solar and geomagnetic activity varies during different solar cycle phases.

1. DATA AND PROCESSING TECHNIQUE

The catalog of enhancements of >30 keV FEE fluxes was compiled from measurements of charged particle fluxes from the open database [<https://ngdc.noaa.gov/stp/satellite/poes/dataaccess.html>] of NOAA/POES and MetOp low-orbit satellites. Table lists the years of operation of each spacecraft (SC). There have been two or

more satellites in orbit since 2001; in 2012 and 2013, there were seven satellites (the maximum number); and in 2023, five SC remained active. Circular polar sun-synchronous orbits have an inclination of 98° at ~ 850 km. The orbital planes occupied from one to three fixed LT ranges including, in particular, terminators (6–18 LT), dawn–dusk (9–21 LT) and night–day (2–14 LT). In 2023, the number of planes was reduced to two and they were unevenly distributed: only one spacecraft remained in the terminator plane, and four in the dawn–dusk plane. Three European MetOp satellites are located in the dawn–dusk plane.

Identical instruments are installed on board all the satellites to measure electron and proton fluxes in a wide range of energies from several eV to hundreds of MeV. This paper is based on data from the MEPED telescope [Evans, Greer, 2006]. It uses pairs of semiconductor detectors with orthogonal orientation, which makes it possible to simultaneously measure fluxes of quasi-trapped and precipitating electrons in three energy channels of the keV range (>30 , >100 , and >300 keV). The vertical detector, aimed at the zenith, records quasi-trapped electrons at low latitudes ($<30^\circ$) and precipitating ones at middle and high latitudes. The horizontal detector along the velocity direction detects particles precipitating at low latitudes and trapped at higher latitudes. Figure 2 shows that electron flux enhancements near the equator are more often recorded by the vertical detector than by the horizontal one. Thus, the flux enhancement at the equator is observed mainly in quasi-trapped electrons [Suvorova et al., 2013]. The work relies on data from the vertical detector in the integral channel $E > 30$ keV

Intervals of satellite fleet operation

Satellites	Years
NOAA-15	1998–present
NOAA-16	2001–2014
NOAA-17	2002–2013
NOAA-18	2005–present
NOAA-19	2009–present
METOP-A	2006–2021
METOP-B	2012–present
METOP-C	2019–present

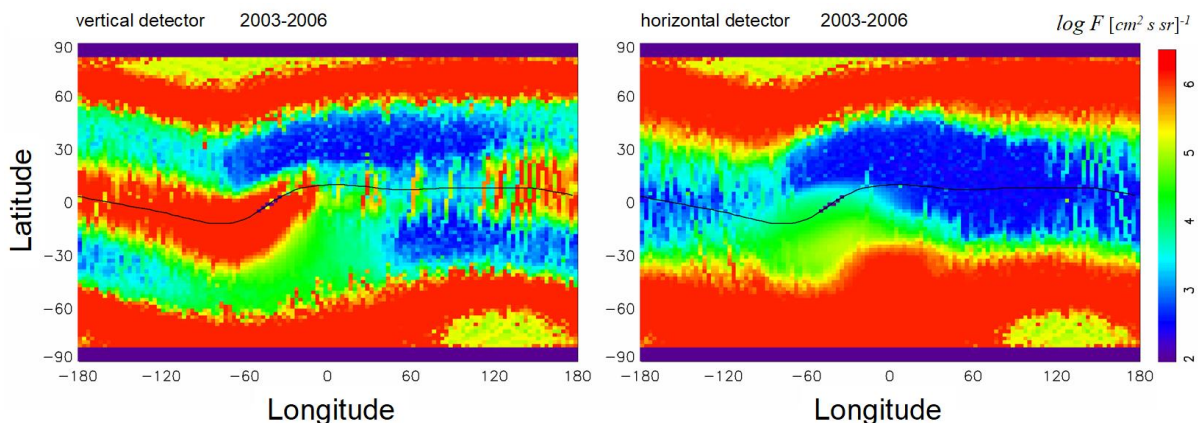


Figure 2. Geographical map of maximum intensity of >30 keV electron fluxes recorded (left) by a vertical detector and (right) by a horizontal detector from 2003 to 2006

for which the statistics on FEE flux enhancements were the most extensive.

Note that the information in the database before 2014 was cleaned of failures and averaged over 16 s. The later information contains raw data with a time resolution of ~ 2 s without pre-filtering numerous failures. Some of the failures we identified as systematic were excluded from processing, as they could distort the results of statistical analysis of FEE fluxes [Golubkov et al., 2024].

FEE flux enhancements at $L < 1.2$ were chosen by visually selecting geographical maps of flux intensities [Suvorova et al., 2012]. The method of constructing intensity maps involved identifying maximum electron fluxes with $E > 30$ keV in spatial cells of $3^\circ \times 2^\circ$ geographical longitude and latitude respectively and for a given time interval, for example, hours or days. The method of determining the maximum flux has an important advantage over the averaging procedure. When averaging data for hundreds or more revolutions, searching for enhancements at low latitudes becomes ineffective since they occur locally and relatively rarely; therefore, background fluxes dominate on long time intervals (days). As a result, the enhancements become

barely noticeable in the averaged map, and maps with maximum fluxes make it possible to effectively detect local transient enhancements of electron fluxes.

The FEE event catalog is a set of geographical maps of >30 keV electron flux intensities per day and a list of dates in 1998–2023 (see Figure 3, *c*). To determine a more accurate time (UT) of each enhancement at the geomagnetic equator, we used time profiles in a dome shape with one maximum (type 1 in Figure 3, *a*). The duration of one enhancement was more than 6 min. Type 2 profiles were not included in the statistics. In the selected events, FEE fluxes at the equator exceeded the background by several orders of magnitude, i.e. from $\sim 10^4$ to 10^7 electrons/($\text{cm}^2 \text{ s sr}$). The dataset for statistical analysis contained the date of the FEE flux enhancement, as well as UT and geographic longitude, referred to the intersection point of the geomagnetic equator (longitudes from -90° to 0° in SAA were excluded). LT was determined from UT and longitude, or from each satellite's data. From the list of events, separate statistics were collected on the number of days in a year, in a month, and statistics on the number of FEE flux enhancements in certain LT periods.

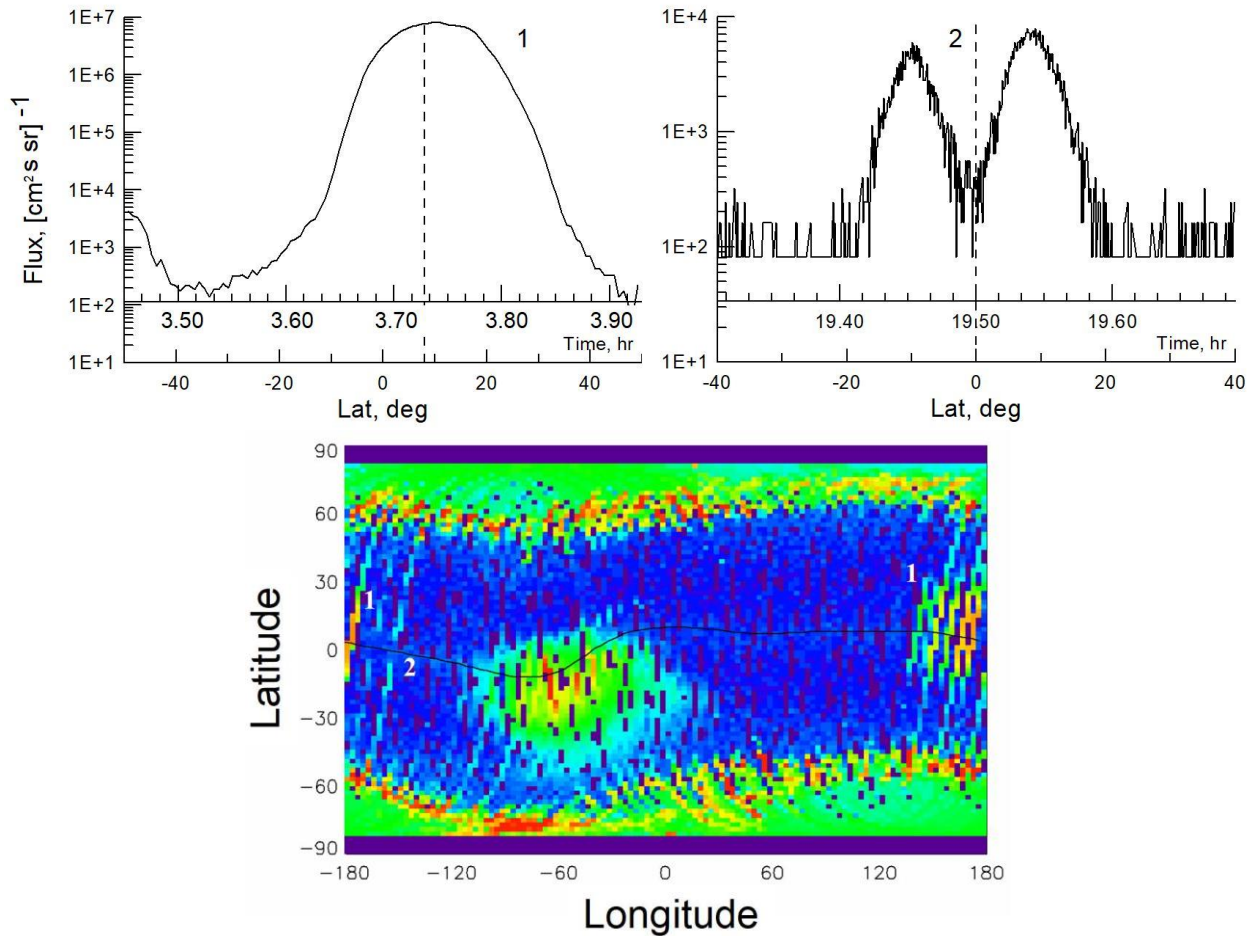


Figure 3. Enhancements of FEE fluxes with electron energy $E_e > 30$ keV: *a* — time profile of the enhancement with one intensity maximum near the equator (type 1); *b* — time profile of the enhancement with two maxima at low latitudes in the Northern and Southern hemispheres and a deep minimum near the equator (type 2). Numbers 1 and 2 mark enhancements of two types. Panel *c* is a global map of maximum intensities for the April 23, 2023 magnetic storm. The geomagnetic equator is indicated by the black curve

2. RESULTS

2.1 Distribution of FEE flux enhancements by local time, months, and years

The LT range was divided into 6 intervals of 4 hrs. Figure 4 illustrates the distribution of FEE flux enhancements by LT. The maximum occurrence rate of the enhancements is within 0–4 LT (mean time is 2 LT). Many events also occur on the adjacent interval 4–8 LT (6 LT). A smaller number, but equally, on the intervals 8–12 (10 LT) and 20–24 LT (22 LT) during the day is the minimum number of FEE flux enhancements. Thus, it is possible to determine the LT sector after midnight (2 LT) to the early morning hours (6 LT), in which the occurrence rate of FEE flux enhancements is the highest; in the daytime, the lowest.

Figure 5 shows the distribution of the number of days with FEE flux enhancements by months. There are two distinct peaks in the distribution: the main one (from May to September) and the secondary one (from December to February). The months of autumn and spring equinoxes correspond to the minimum number of events.

Figure 6 illustrates year distribution of the number of days with FEE flux enhancements. If we omit the first three years (1998–2000) when there was only one satellite in orbit, the cyclicity with a period 10–12 years is clearly visible in the distribution. One maximum occurred from 2005 to 2008; the second, from 2017 to 2019, which corresponds to the declining and minimum phases of solar cycles 23 and 24 respectively. Minimum occurrence rates of FEE flux enhancements were observed in 2002 and 2014, which is peculiar to the maximum phases of the cycles.

2.2. Geomagnetic activity during FEE events

Geomagnetic activity is responsible for the dynamics of the entire magnetosphere and, in turn, is controlled by solar activity and solar wind (SW). We have selectively compared the daily maps from the FEE catalog with the level of geomagnetic activity [<https://wdc.kugi.kyoto-u.ac.jp/aeasy/index.html>]. In particular, we took events in which the fluxes had a very high intensity ($>10^5$ electrons/(cm² s sr)). It turned out that during the FEE events the level of geomagnetic activity might have been arbitrary, including magnetic storms, substorms, and quiet conditions. The maximum intensity of FEE fluxes recorded per day did not depend on the storm/substorm strength. Moreover, under similar geomagnetic conditions, for example, the same *Dst* index at the maximum of a magnetic storm, flux enhancements could occur or not. For example, there were no FEE flux enhancements during some strong magnetic storms (K_p could increase to 8, and *Dst* could drop below -200 nT), given as examples in [Suvorova, Dmitriev, 2015]. On the contrary, under very quiet conditions ($K_p \leq 1$), FEE fluxes were observed for several hours [Suvorova et al., 2019]. Detailed analysis of this case has revealed a connection with plasma pressure pulses that were generated in a foreshock in the subsolar region for the quasi-radial interplanetary magnetic field

(IMF). Figures 7 and 8 show several cases inconsistent with the typical dependence on geomagnetic activity. There were no FEE flux enhancements (see Figure 7) during a series of strong magnetic storms ($|Dst| \sim 150$ and ~ 200 nT) from September 30 to October 3, 2001 and during the October 22, 2022 moderate storm ($|Dst| \sim 90$ nT). These storms occurred in the maximum phase of cycle 23 and in the rising phase of cycle 25. On the other hand, long-term FEE fluxes were observed on August 1, 2008 and May 16, 2020 under very quiet conditions (see Figure 8) during minimum phases of cycles 23 and 24. Auroral activity was also very low, which is clearly seen on the map as very weak local precipitation of energetic electrons from outer ERB at latitudes above 60° .

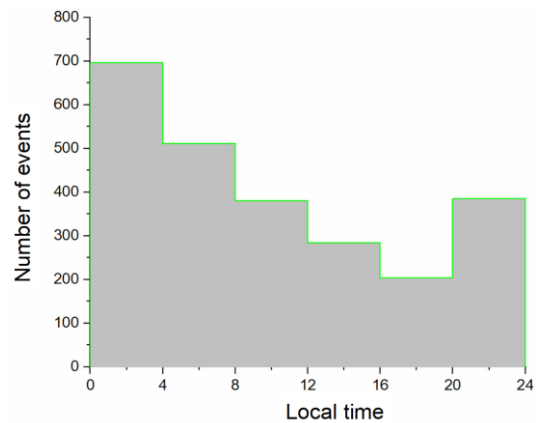


Figure 4. FEE distribution by LT

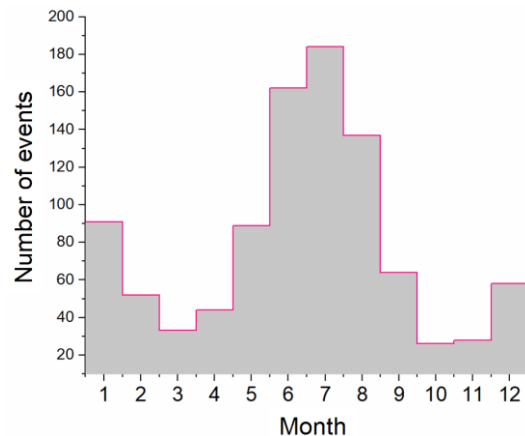


Figure 5. The same by months

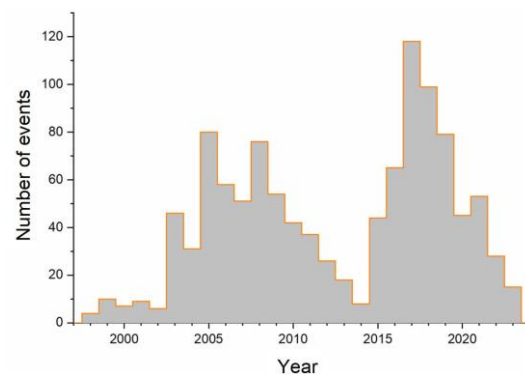


Figure 6. The same by years

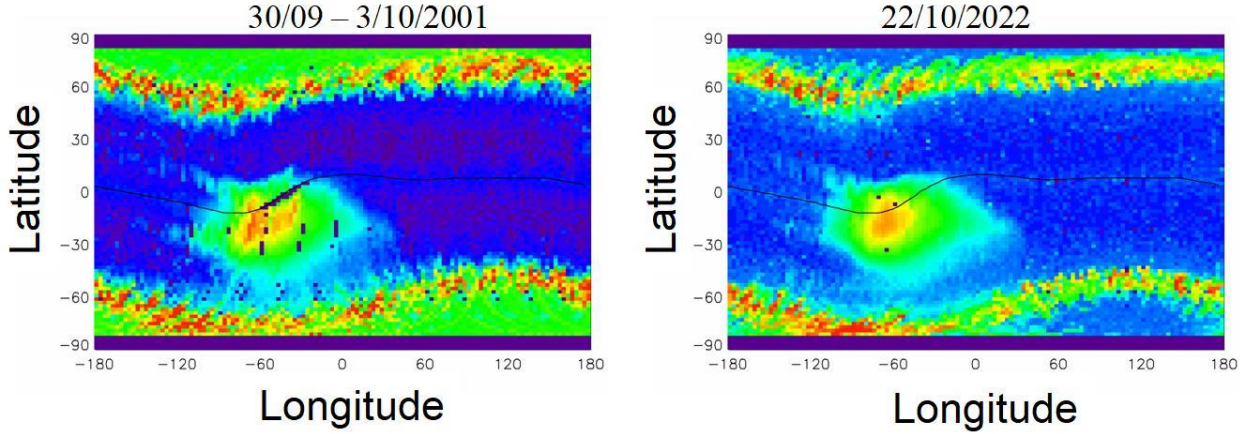


Figure 7. Geographical maps of the intensity of electron fluxes with energy >30 keV during geomagnetic storms on September 30 – October 3, 2001 (a) and October 22, 2022 (b). In these events, there were no FEE flux enhancements in the forbidden zone

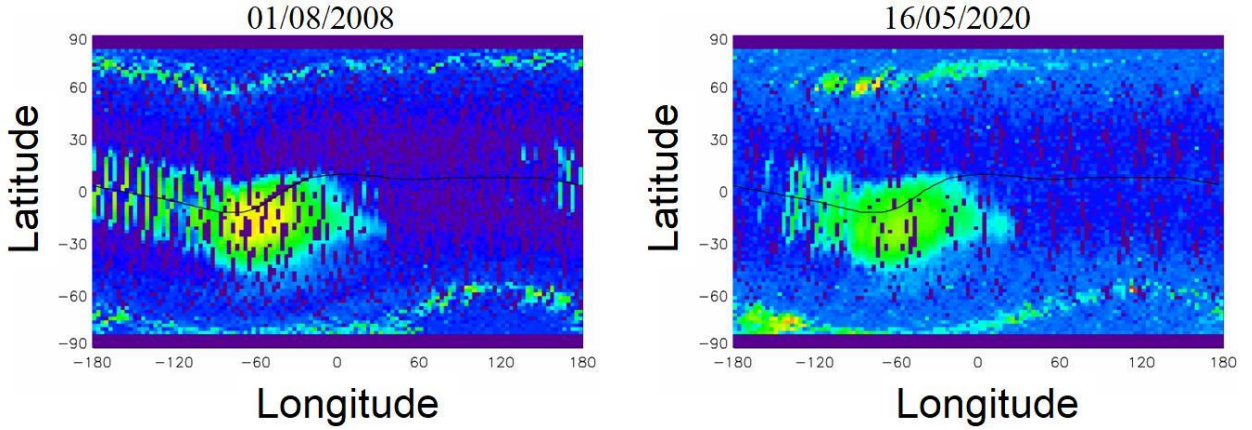


Figure 8. Geographical maps of the intensity of electron fluxes under quiet geomagnetic conditions ($K_p \sim 0-2$) on August 1, 2008 and May 16, 2020. In these events, FEE flux enhancements were observed in the forbidden zone for several hours

2.3. Solar activity and solar wind during FEE events

We have explored how solar activity and SW parameters [<https://omniweb.gsfc.nasa.gov/>] affect the FEE occurrence rate. Correlation coefficients have been calculated between the annual rate of FEE occurrence (see Figure 6) and annual average $F10.7$, Alfvén Mach number M_A , SW plasma velocity V , density D , temperature T , and IMF strength B . We have found out that there is a strong connection with $F10.7$ ($c=-0.77$) and M_A ($c=0.70$), as well as a significant relationship with IMF B ($c=-0.5$); yet for the other parameters the correlation coefficients did not exceed 0.2. For the log-log dependence, the correlation coefficients increased significantly: for $F10.7$ $c=-0.87$, for M_A $c=0.76$. While the SW plasma parameters taken separately did not show any connection with the FEE events, V , D , and B together affect the FEE occurrence since they are included in the expression for the Mach number. Figure 9 illustrates variations in the FEE occurrence rate and annual average $F10.7$ and M_A for the period from 1998 to 2023 considered. It is worth noting that the FEE occurrence rate anticorrelates with $F10.7$ and correlates with M_A . We have also included in the analysis another parameter

proposed in [Borovsky, Birn, 2014] to estimate the rate of local reconnection at the dayside magnetopause. The expression for R (see (8) in [Borovsky, Birn, 2014]) contains almost all SW parameters (M_A , V , D) except T . The correlation coefficient $c=-0.34$ between the FEE occurrence rate and R proved to be quite low — this does not contradict the empirical fact that magnetic storms do not always give rise to FEE.

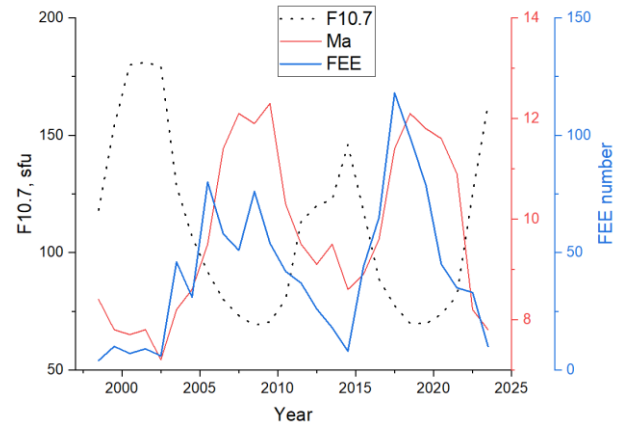


Figure 9. Variations in the occurrence rate of FEE events, annual average $F10.7$ and M_A in 1998–2023

3. DISCUSSION

In this paper, we have examined one of the aspects of the ERB electron dynamics on low drift L shells: sporadic enhancements of energetic electron (FEE) fluxes in the forbidden zone ($L < 1.2$). The source of large FEE fluxes is known to be inner ERB [Suvorova et al., 2014]. Which physical mechanism provides the FEE flux enhancement is the main question in this problem. Various mechanisms were proposed at different times, but more and more often opinions agree that dynamic phenomena in and under the inner belt may be related by a common process, namely, radial transport or fast particle drift toward Earth [Suvorova et al., 2012, 2013; Lejosne, Mozer, 2016; Selesnick et al., 2016, 2019; Su et al., 2016]. The radial transport of particles occurs in crossed magnetic and electric fields; with the westward direction of the electric field, the drift is earthward. Thus, the electric field plays a key role in the radial transport of particles, but it is necessary to determine sources of this field or the local mechanism of its generation at ~ 1000 – 1500 km near the equator. To date, this problem has not yet been solved [Su et al., 2016] since the principle of electric field shielding in the inner zone ($L < 3$) underlies electrodynamic models, i.e. the electric field of enhanced magnetospheric convection does not penetrate to low latitudes and altitudes.

In the case of transient enhancements of FEE fluxes, the events can be interpreted as injections, and this requires a fairly strong electric field (\sim several mV/m) at low latitudes and altitudes of ~ 1000 km [Suvorova et al., 2014; Suvorova, Dmitriev, 2015]. However, with modern electrodynamic models [Su et al., 2016] it is difficult to justify even minor deviations of the electric field from the average 0.4 – 1 mV/m on low L shells [Selesnick et al., 2016]. In [Hua et al., 2019; Hui, Vichare, 2019; Lejosne, Mozer, 2016; Lejosne et al., 2021, 2022; Selesnick et al., 2016], various sources of electric field, including ionospheric and magnetospheric ones, are proposed for modeling radial drift in the inner belt. According to theoretical estimates [Selesnick et al., 2019], an electric field of ~ 5 mV/m is needed to explain observations of deep injections of electrons from inner ERB into low L shells. In these papers, it is noted that it is necessary to figure out how electric fields penetrate from high latitudes to the equator and what role field-aligned currents can play in this process.

In the presented statistical study of enhancements of keV electron fluxes in the forbidden zone, we have found out which external conditions are necessary to initiate injection in the $L < 1.2$ region, and which may be an optional addition. The first factors include solar activity and SW; the second, geomagnetic activity. We have shown that there is no unambiguous connection with magnetic storms and correlation with the local rate of daily reconnection. On the other hand, we have demonstrated that FEE events can also occur under quiet conditions. These results are in line with those obtained in [Suvorova, 2017], where it has been shown that FEE occurrence does not depend on the substorm activity index AL and the induced interplanetary electric field, i.e. the IMF B_z component.

Note that the absence of a connection between FEE events and geomagnetic activity may also indicate an alternative source of energetic electrons not from ERB, but from the lower atmosphere during thunderstorm activity. Given the geographical distribution of thunderstorm activity, the maximum expectation of FEE events is assumed to be in the equatorial region in the longitude sector over Southeast Asia and Oceania, which is consistent with observational statistics, but only partially. Nevertheless, the events are observed much more often over the Pacific Ocean in the Western Hemisphere [Suvorova, 2017]. It is a fair indication that in the case of thunderstorm activity such events should not depend on solar cycle, but occur more often in the afternoon and in the summer. From our point of view, the validity of this hypothesis is denied by the results of statistical analysis in which LT distributions of the events have a maximum in the night hours, two maxima in the seasonal distribution (winter and summer), and an obvious solar-cyclic variation. We, therefore, argue for the mechanism of fast radial transport (injection type) from the inner ERB.

Suvorova [2017] has hypothesized that the solar illumination of the polar ionosphere and the conductivity in the auroral region play an important role in the occurrence of FEE. The summer months of the Northern Hemisphere just provide the most suitable conditions for solar illumination and high conductivity of the polar cap and the dayside oval; the winter months create similar conditions in the Southern Hemisphere with the only difference that the area of the illuminated polar region is smaller due to the asymmetry and the dipole tilt. The seasonal distribution of FEE is likely to exhibit the effect of uneven ionospheric conductivity in the auroral zone in combination with the dipole tilt [Suvorova, 2017].

The LT distribution of FEE events is maximum at 2–6 LT, i.e. electrons are injected more often in the post-midnight sector. In the night and early morning hours, the residual ionospheric conductivity in the subauroral region is very low [Liu, Chen, 2009], which we consider an important factor. In this case, the large difference between the conductivities of the day and night ionosphere can be assumed to contribute to more effective penetration of electric field disturbances from high latitudes deep into the inner magnetosphere, mainly in the after-midnight sector. This hypothesis allows us to interpret the results of the correlation analysis as follows.

1. We have found that FEE injections anticorrelate with $F10.7$, which, in turn, correlates well with the solar cycle [Clette, 2021]. The $F10.7$ index controls ionization of the dayside ionosphere. In terms of ionospheric conductivity this means that during solar minimum ionization of the dayside ionosphere is on average much lower than that at solar maximum. On the other hand, the maximum phase is characterized by disturbed conditions in SW, which lead to high geomagnetic activity and intensification of precipitation of charged particles into the night auroral ionosphere. Since, as a consequence, night ionization increases significantly at high latitudes, the difference between day and night ionization decreases on average and then the efficiency of electric field penetration to low latitudes goes down.

The number of electron injections, therefore, decreases at solar maximum and this is expressed in the anticorrelation between $F10.7$ and the rate of FEE occurrence. At solar minimum, particles precipitate less frequently and have a lower flux intensity, so ionization of the night ionosphere is very low. Of special note is that in the after-midnight hours in the absence of additional sources of ionization recombination processes lead to the fact that the electron density is at least by an order of magnitude lower than in the dayside ionosphere. Even a decrease in ionization of the dayside ionosphere due to a 2–3-fold decrease in $F10.7$ at solar minimum relative to solar maximum cannot compensate for the resulting large difference (10-fold) between the dayside and nightside ionosphere, which enables penetration of an electric field.

2. We have found that FEE injections correlate with M_A of SW plasma. Auroral activity, namely the occurrence rate of substorms, decreases with increasing M_A and becomes maximum during the declining phase of solar cycle [Borovsky, Yakimenko, 2017]. Thus, M_A is also responsible for the conductivity of the nightside auroral ionosphere: large M_A means that substorms are rarer and the conductivity is lower. In terms of ionospheric conductivity this means that at solar minimum the occurrence rate of substorms and the ionization of the nightside ionosphere are on average lower than in other solar cycle phases, i.e. here we can see that an important condition for penetration of the electric field is the low conductivity of the nightside ionosphere in the auroral/subauroral region. Higher residual conductivity in the nightside auroral region, for example, due to frequent substorms and storms, can restrain penetration of the electric field from high latitudes to the equator.

CONCLUSION

Statistical analysis of FEE events performed on the basis of the catalog has revealed solar-cyclic, as well as seasonal and diurnal variations in the occurrence of FEE enhancements. We have examined the correlation of the annual occurrence rate of FEE events with solar activity, SW parameters, and geomagnetic activity. Strong correlations have been found between FEE events, $F10.7$, and M_A . We have proposed an interpretation of the results based on the mechanism of electric drift and radial electron transport from the inner ERB to the forbidden zone ($L < 1.2$). We have drawn a conclusion that the key factor in the mechanism is the effective penetration of the electric field to low latitudes. The most suitable penetration conditions appear when there is a significant difference between the conductivities of the high-latitude ionosphere in the solar illuminated and unilluminated (after-midnight) LT sectors and a decrease in the occurrence rate of substorms.

We are grateful to the creators of the databases OMNI (Goddard Space Flight Center, NASA, USA) and NOAA/POES (National Centers for Environmental Information, NOAA, USA) for the opportunity to use the data in this study.

The work was carried out under the research theme “Solar research, monitoring, and modeling of the radiation environment and plasma processes in the heliosphere and geospace”.

REFERENCES

- Asikainen T., Mursula K. Filling the South Atlantic anomaly by energetic electrons during a great magnetic storm. *Geophys. Res. Lett.* 2005, vol. 32, L16102. DOI: [10.1029/2005GL023634](https://doi.org/10.1029/2005GL023634).
- Borovsky J.E., Birn J. The solar wind electric field does not control the dayside reconnection rate. *J. Geophys. Res.: Space Phys.* 2014, vol. 119, pp. 751–760. DOI: [10.1002/2013JA019193](https://doi.org/10.1002/2013JA019193).
- Borovsky J.E., Yakymenko K. Substorm occurrence rates, substorm recurrence times, and solar wind structure. *J. Geophys. Res.: Space Phys.* 2017, vol. 122, pp. 2973–2998. DOI: [10.1002/2016JA023625](https://doi.org/10.1002/2016JA023625).
- Clette F. Is the $F_{10.7\text{cm}}$ — sunspot number relation linear and stable? *J. Space Weather Space Clim.* 2021, vol. 11, iss. 5, art. 2. DOI: [10.1051/swsc/2020071](https://doi.org/10.1051/swsc/2020071).
- Dmitriev A.V., Yeh H.-C. Storm-time ionization enhancements at the topside low-latitude ionosphere. *Ann. Geophys.* 2008, vol. 26, pp. 867–876.
- Evans D.S. Dramatic increases in the flux of >30 keV electrons at very low L -values in the onset of large geomagnetic storms. *EOS Trans.* 1988, vol. 69, iss. 44, pp. 1393.
- Evans D.S., Greer M.S. Polar Orbiting Environmental Satellite Space Environment Monitor – 2: *Instrument descriptions and archive data documentation*. 2006. available from NGDC: <http://ngdc.noaa.gov/stp/satellite/poes/documentation.html> (accessed April 25, 2024).
- Golubkov M.G., Suvorova A.V., Dmitriev A.V., et al. Statistical analysis of decreases in energetic electron fluxes in low-latitude ionosphere from NOAA/POES and MetOp 1998–2022 data. *Russian J. Physical Chemistry B: Focus on Physics*. 2024, vol. 43. (In print).
- Gusev A., Kohno T., Martin I., Pugacheva G.I., Turtelli A. Jr., Tyka A.J., Kudela K. Injection and fast radial diffusion of energetic electrons into the inner magnetosphere. *Planet. Space Sci.* 1995, vol. 43, pp. 1131–1134.
- Heikkilä W.J. Soft particle fluxes near the equator. *J. Geophys. Res.* 1971, vol. 76, pp. 1076–1078.
- Hua M., Li W., Ma Q., Binbin Ni1, Nishimura Y., Shen Xiao-Chen, Li H. Modeling the electron enhancement and butterfly pitch angle distributions on L shells < 2.5 . *Geophys. Res. Lett.* 2019, vol. 46, pp. 10967–10976. DOI: [10.1029/2019GL084822](https://doi.org/10.1029/2019GL084822).
- Hui D., Vichare G. Variable responses of equatorial ionosphere during undershielding and overshielding conditions. *J. Geophys. Res.: Space Phys.* 2019, vol. 124, pp. 1328–1342. DOI: [10.1029/2018JA025999](https://doi.org/10.1029/2018JA025999).
- Imhof W.L., Gaines E.E., Reagan J.B. Dynamic variations in intensity and energy spectra of electrons in the inner radiation belt. *J. Geophys. Res.* 1973, vol. 78, pp. 4568–4576. DOI: [10.1029/ja078i022p04568](https://doi.org/10.1029/ja078i022p04568).
- Kudela K., Matisin J., Shuiskaya F.K., Akentieva O.S., Romantsova T.V., Venkatesan D. Inner zone electron peaks observed by the “Active” satellite. *J. Geophys. Res.* 1992, vol. 97, pp. 8681–8683.
- Lejosne S., Mozer F.S. Typical values of the electric drift $E \times B / B^2$ in the inner radiation belt and slot region as determined from Van Allen Probe measurements. *J. Geophys. Res.: Space Phys.* 2016, vol. 121, pp. 12014–12024. DOI: [10.1002/2016JA023613](https://doi.org/10.1002/2016JA023613).
- Lejosne S., Fedrizzi M., Maruyama N., Selesnick R.S. Thermospheric neutral winds as the cause of drift shell distur-

tion in Earth's inner belt. *Front. Astron. Space Sci.* 2021, vol 8, art. 725800. DOI: [10.3389/fspas.2021.725800](https://doi.org/10.3389/fspas.2021.725800).

Lejosne S., Fejer B., Maruyama N., Scherliess L. Radial transport of energetic electrons as determined from the “zebra stripes” measured in the Earth's inner belt and slot region. *Front. Astron. Space Sci.* 2022, vol. 9, art. 823695. DOI: [10.3389/fspas.2022.823695](https://doi.org/10.3389/fspas.2022.823695).

Liu L., Chen Y. Statistical analysis of solar activity variations of total electron content derived at Jet Propulsion Laboratory from GPS observations. *J. Geophys. Res.: Space Phys.* 2009, vol. 114, A10311. DOI: [10.1029/2009JA014533](https://doi.org/10.1029/2009JA014533).

Paulikas G.A. Precipitation of particles at low and middle latitudes. *Rev. Geophys. Space Phys.* 1975, vol. 13, iss. 5, pp. 709–734.

Pinto O., Pinto R.C.A., Gonzalez W.D., Gonzalez A.L.C. About the origin of peaks in the spectrum of inner belt electrons. *J. Geophys. Res.* 1991, vol. 96, pp. 1857–1860. DOI: [10.1029/90JA02383](https://doi.org/10.1029/90JA02383).

Sauvaud J.A., Moreau T., Maggiolo R., Treilhou J.-P. High-energy electron detection onboard DEMETER: The IDP spectrometer description and first results on the inner belt. *Planet. Space Sci.* 2006, vol. 54, pp. 502–511.

Savenko I.A., Shavrin P.I., Pisarenko N.F. Low-energy particles at heights of 320 km and at near-equator latitudes. *Iskusstvennye sputniki Zemli* [Artificial Earth Satellites]. 1962, no. 3, pp. 75–80. (In Russian).

Selesnick R.S., Su Y.-J., Blake J.B. Control of the innermost electron radiation belt by large-scale electric fields. *J. Geophys. Res.: Space Phys.* 2016, vol. 121, pp. 8417–8427. DOI: [10.1002/2016JA022973](https://doi.org/10.1002/2016JA022973).

Selesnick R.S., Su Y.-J., Sauvaud J.A. Energetic electrons below the inner radiation belt. *J. Geophys. Res.: Space Phys.* 2019, vol. 124, pp. 5421–5440. DOI: [10.1029/2019JA026718](https://doi.org/10.1029/2019JA026718).

Su Y.-J., Selesnick R.S., Blake J.B. Formation of the inner electron radiation belt by enhanced large-scale electric fields. *J. Geophys. Res.: Space Phys.* 2016, vol. 121, pp. 8508–8522. DOI: [10.1002/2016JA022881](https://doi.org/10.1002/2016JA022881).

Sun W., Yang J., Wang W., Cui J., Toffoletto F., Yue C., et al. Archimedean spiral distribution of energetic particles in Earth's inner radiation belt. *Geophys. Res. Lett.* 2024, vol. 51, e2023GL106859. DOI: [10.1029/2023GL106859](https://doi.org/10.1029/2023GL106859).

Suvorova A.V. Flux enhancements of >30 keV electrons at low drift shells $L < 1.2$ during last solar cycles. *J. Geophys. Res.: Space Phys.* 2017, vol. 122, pp. 12274–12287. DOI: [10.1002/2017JA024556](https://doi.org/10.1002/2017JA024556).

Suvorova A.V., Dmitriev A.V. Radiation aspects of geomagnetic storm impact below the radiation belt. *Cyclonic and Geomagnetic Storms: Predicting Factors, Formation and Environmental Impacts*. New York: NOVA Science Publishers, 2015, pp. 19–76.

Suvorova A.V., Tsai L.C., Dmitriev A.V. On relation between mid-latitude ionospheric ionization and quasi-trapped energetic electrons during 15 December 2006 magnetic storm. *Planet. Space Sci.* 2012, vol. 60, pp. 363–369. DOI: [10.1016/j.pss.2011.11.001](https://doi.org/10.1016/j.pss.2011.11.001).

Suvorova A.V., Dmitriev A.V., Tsai L.-C., Kunitsyn V.E., Andreeva, E.S. Nesterov I.A., Lazutin L.L. TEC evidence for near-equatorial energy deposition by 30 keV electrons in the topside ionosphere. *J. Geophys. Res.* 2013, vol. 118, pp. 4672–4695. DOI: [10.1002/jgra.50439](https://doi.org/10.1002/jgra.50439).

Suvorova A.V., Huang C.-M., Matsumoto H., Dmitriev A.V., Kunitsyn V.E., Andreeva E.S., et al. Low-latitude ionospheric effects of energetic electrons during a recurrent magnetic storm. *J. Geophys. Res.: Space Phys.* 2014, vol. 119, pp. 9283–9302. DOI: [10.1002/2014JA020349](https://doi.org/10.1002/2014JA020349).

Suvorova A.V., Dmitriev A.V., Parkhomov V.A., Tsegmed B. Quiet time structured Pc1 waves generated during transient foreshock. *J. Geophys. Res.: Space Phys.* 2019, vol. 124, pp. 9075–9093. DOI: [10.1029/2019JA026936](https://doi.org/10.1029/2019JA026936).

Tadokoro H., Tsuchiya F., Miyoshi Y., Misawa H., Morioka A., Evans D.S. Electron flux enhancement in the inner radiation belt during moderate magnetic storms. *Ann. Geophys.* 2007, vol. 25, pp. 1359–1364.

Takagi S., Nakamura T., Kohno T., Shiono N., Makino F. Observation of space radiation environment with EXOS-D. *IEEE Trans. Nucl. Sci.* 1993, vol. 40, iss. 6, pp. 1491–1497.

Tanaka Y., Nishino M., Iwata A. Magnetic storm-related energetic electrons and magnetospheric electric fields penetrating into the low-latitude magnetosphere ($L \sim 1.5$). *Planet. Space Sci.* 1990, vol. 38, iss. 8, pp. 1051–1059.

URL: <https://omniweb.gsfc.nasa.gov/> (accessed April 25, 2024).

URL: <https://ngdc.noaa.gov/stp/satellite/poes/dataaccess> (accessed April 25, 2024).

URL: <https://wdc.kugi.kyoto-u.ac.jp/aeasy/index.html> (accessed April 25, 2024).

This paper is based on material presented at the 19th Annual Conference on Plasma Physics in the Solar System, February 5–9, 2024, IKI RAS, Moscow.

Original Russian version: Suvorova A.V., Dmitriev A.V., published in *Solnechno-zemnaya fizika*. 2024. Vol. 10. No. 3. P. 79–87. DOI: [10.12737/szf-103202409](https://doi.org/10.12737/szf-103202409). © 2024 INFRA-M Academic Publishing House (Nauchno-Izdatelskii Tsentr INFRA-M)

How to cite this article

Suvorova A.V., Dmitriev A.V. Conditions for the occurrence of intense fluxes of energetic electrons at $L < 1.2$ associated with solar activity and solar wind parameters. *Solar-Terrestrial Physics*. 2024. Vol. 10. Iss. 3. P. 75–82. DOI: [10.12737/stp-103202409](https://doi.org/10.12737/stp-103202409).